JOURNAL OF MATERIALS SCIENCE 27 (1992) 4678–4684

Non-linear properties of polymer cellular materials with a negative Poisson's ratio

J. B. CHOI*, R. S. LAKES
*Department of Mechanical Engineering, *Department of Biomedical Engineering, and Center for Laser Science and Engineering, University of Iowa, Iowa City, IA 52242, USA*

Negative Poisson's ratio polymeric cellular solids (re-entrant foams) were studied to ascertain the optimal processing procedures which give rise to the smallest value of Poisson's ratio. The non-linear stress–strain relationship was determined for both conventional and re-entrant foams; it depended upon the permanent volumetric compression achieved during the processing procedure. Poisson's ratio of re-entrant foam measured as a function of strain was found to have a relative minimum at small strains. The toughness of re-entrant foam increased with permanent volumetric compression, and hence with density.

1. Introduction

Almost all ordinary materials undergo a lateral contraction when stretched and a lateral expansion when compressed. Poisson's ratio is defined as the negative of the lateral strain divided by the longitudinal strain when a load is applied in the longitudinal direction. Therefore, all ordinary materials exhibit a positive Poisson's ratio, including ordinary cellular solids [1].

The question of how much freedom is associated with elastic solids has been an open one from the earliest development of elastic theory. For example, the early "uni-constant" elasticity theory proposed by some of the early founders of the theory of elasticity, and based on a model of central force interatomic interaction [2, 3], predicts the shear modulus to be two-fifths of Young's modulus and Poisson's ratio to be 1/4 for all solids. The failure of the uni-constant theory followed from experimental work in the late 1800s which disclosed values of Poisson's ratio close to 1/3 for common structural materials. These experiments led to the acceptance of the classical elasticity theory used today. The allowable range of Poisson's ratio for an isotropic elastic material is -1.0 to $+0.5$. Negative Poisson's ratios are sufficiently unusual that some writers present an allowable range of 0 to 0.5, but they are not entirely unknown. Such effects have been reported in single-crystal pyrites [3] and in some rocks [4]. Recently, a method to make a foam material having a negative Poisson's ratio was developed by one of the authors [5]. It involved a transformation of the cell structure from a convex polyhedral shape to a concave or "re-entrant" shape [5]. This transformation was achieved by heating the foam to its softening point while triaxially compressed such that the deformation would remain after cooling. Recently it has been shown that other synthetic microstructures can give rise to negative Poisson's ratios [6–8], albeit in the presence of much anisotropy.

Applications of negative Poisson's ratio materials may be envisaged in relation to the Poisson's ratio itself or in relation to other material properties which arise from the unusual structure. Furthermore, from the relation $G = E/2(1 + \nu)$ between the Young's modulus E, the shear modulus G and Poisson's ratio ν, when Poisson's ratio approaches -1, the shear modulus substantially exceeds the Young's modulus. By contrast, the Young's modulus of ordinary materials is two to three times larger than the shear modulus. Negative Poisson's ratio materials may offer advantages in terms of damage resistance, in view of modification of stress concentration factors for inhomogeneities. Stress concentration factors are reduced for cavities when $\nu < 0$; they are increased for inclusions [9, 10]. Similarly, plane strain fracture toughness [5] is predicted to be improved by a negative Poisson's ratio. Negative Poisson's ratio materials also exhibit superior effective mechanical properties such as resilience. Various applications of materials with negative Poisson's ratio may be envisaged on the basis of their properties; specific applications will be presented elsewhere.

In this article we present results for optimal re-entrant foam processing conditions of temperature, time of processing, and permanent volumetric compression; and the non-linear mechanical properties of the conventional and re-entrant foams.

2. Experimental procedure

2.1. Rationale

There are many factors which may influence the creation of re-entrant foams with negative Poisson's ratio, including the starting material composition, temperature, time of processing, humidity, permanent volumetric compression ratio, relative density ρ/ρ_s (the density of the cellular material, ρ, divided by that of the solid, ρ_s), cell size and so on. In this study two

0022–2461

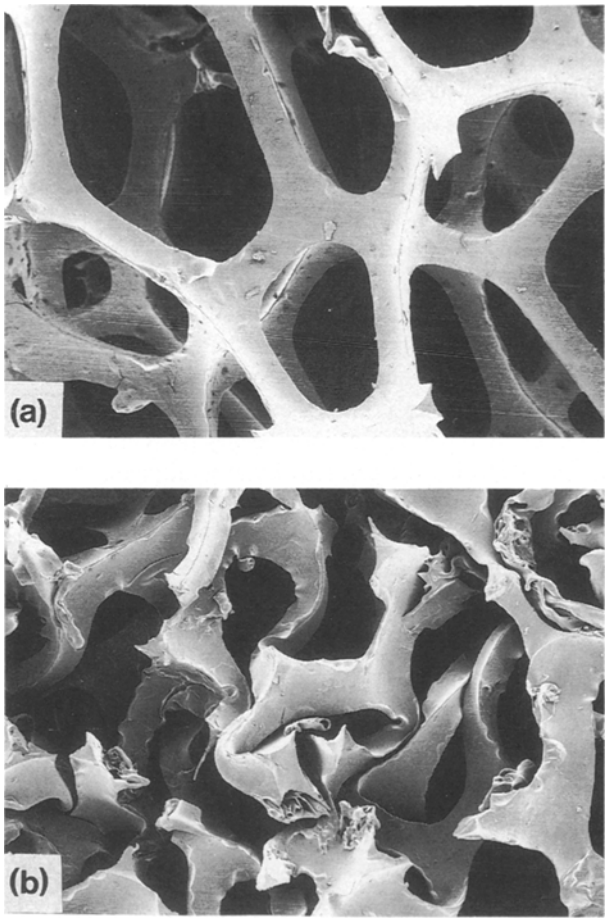

Figure 1 Scanning electron micrographs of Scott foam: (a) conventional foam, (b) re-entrant foam, permanent volumetric compression ratio 3.2. Magnification × 25.

kinds of polymer foam were examined, and several of the processing variables explored.

2.2. Materials

Materials used included a grey polyurethane–polyester foam ($\rho/\rho_s = 0.03 \pm 10\%$, L (length of cell rib) = 0.4 $\pm$ 0.03 mm) obtained from Clark Foam Inc. in Coralville, Iowa. This foam is partly closed and partly open cell, as shown microscopically by Friis *et al.* [11]. Scott industrial foam ($\rho/\rho_s = 0.03 \pm 7\%$, $L = 1.2 \pm 0.03$ mm) was obtained from Foamade Industries, Auburn Hills, Michigan. It is a reticulated foam with all open cells (Fig. 1). The foams were cut into long bars of square cross-section. They exhibited some variation in the relative density in each bar; however, the variation was considered negligble.

2.3. Materials processing

The experimental procedure was as follows. The furnace was preheated to the predetermined temperature. A square aluminium tube (inner dimensions 22 mm × 22 mm × 125 mm) was used as a mould for the foam which was cut oversize (38 mm × 38 mm × 125 mm in the case of the grey foam). For the grey foam, the inner walls were lubricated with a vegetable oil to aid in the insertion of the foam. The foam was inserted into the tube with the aid of a tongue depressor to eliminate surface wrinkles; this procedure gave compression in two transverse directions. End-plates 2.1 mm thick and spacer tubes 23 mm long were then inserted into the mould, and were compressed with a clamping device to compress the foam in the third, longitudinal, direction. The foam and mould assembly was placed in the furnace for a predetermined time. The specimen was then cooled at room temperature for 10 min, and was removed from the mould. The specimen was then stretched in each of three orthogonal directions to eliminate any adhesion of the ribs.

All the experiments using grey polyurethane foam were performed using an equal initial volumetric compression ratio of 5.0. Since this material exhibited considerable recovery, the processing time and temperature were varied to control the final volumetric compression ratio. Scott industrial foam was transformed for 17 min at 170 °C, a combination found to be near optimal in previous studies. The final volumetric compression ratio was controlled by preparing different size starting blocks.

2.4. Grey foam test

Grey foam specimens were cut into 30 mm long and 10 mm × 10 mm cross-section pieces. The pieces chosen were those which showed the best negative effect in Poisson's ratio; the best portion was usually near the end portion of the block. In order to measure longitudinal and lateral strain, two lines 10 mm apart were drawn in the middle of the lateral surface and the foam was bonded to a straining apparatus with cyanoacrylate cement. The longitudinal strain was changed by 5% and lateral deformation was measured with a micrometer; the measurement was made 3 to 5 s after application of the load to minimize viscoelastic effects.

2.5. Scott foam test

For this study, specimens were cut from a block of re-entrant foam according to the ASTM standard for both tension and compresssion tests [12, 13]. The tension specimens were 50 mm long and 12.5 mm × 12.5 mm in cross-section, with a gauge length of 40 mm. The compression specimens were 10 mm long and 12.5 mm × 12.5 mm in cross-section to avoid buckling.

For the tension test, the specimen was bonded to the test machine fixtures with cyanoacrylate cement. In preliminary compression tests, Teflon tape was used between the specimen and the loading surface to reduce the lateral bulging or concavity due to the friction force on the contact surfaces combined with the Poisson effect. This procedure led to errors in initial seating stress since the foam specimens could not be made perfectly flat as a result of their heterogeneous structure. Consequently for compression tests, the two surfaces were bonded together as in the case of the tension test.

A servohydraulic testing machine (MTS Corp.) with a 2.5 kN load cell was used to load the specimens. The gains for the load and displacement channels were controlled during the test in order to obtain data for

small and large strain. Standard methods which utilize strain gauges or dial gauges cannot be used in this experiment due to the compliance of the foam. Therefore, measurements of axial and transverse deformation were made using magnified images derived from a video camera. Experiments were performed at a constant displacement rate of 0.2/mm s^{-1} and at a room temperature of 20 ± 2 °C.

Both polymer foams are viscoelastic materials which may have some dependence upon temperature and strain rate. Independent experiments at small strain disclosed a loss tangent from 0.05 to 0.1 between 0.1 and 10 Hz, sufficiently small that viscoelastic effects should not be a problem in the interpretation of the current experiments.

3. Results and discussion

For the grey polyurethane foam, the initial volumetric compression ratio was 5, however the foam recovered so that the final compression ratio was less. Fig. 2 shows the volumetric compression ratio after recovery as it depends on processing time duration and temperature. Fig. 2 also shows the range of processing conditions leading to a good negative Poisson's ratio effect. A good negative Poisson's ratio effect was also produced by processing at 150 °C for 40 min and at 190 °C for 13 and 14 min. The latter produced a desirable effect without any adhesion of the ribs, but, after a few days, a considerable amount of recovery occurred and the Poisson's ratio was no longer negative. As shown in Fig. 2, the best results were obtained for a final volumetric compression ratio of 3.3 to 3.7. For times and temperatures higher than optimum, corresponding to larger final volumetric compressions, the foam ribs were excessively stuck together. For times and temperatures lower than optimum, resulting in smaller final volumetric compressions, there was a large amount of recovery following treatment, and the negative Poisson's ratio effect was not very pronounced.

The Scott industrial foam was processed at 170 °C for 17 min, a procedure found to be satisfactory in prior tests, and also near the optimum for the grey foam. Re-entrant Scott foam is shown in Fig. 1. The Scott foam was easier to process than the grey foam; it exhibited less adhesion of the ribs and was less sensitive to processing time and temperature. The Scott foam processed in this way recovered 5% or less in volume.

Fig. 3 shows the Poisson's ratio versus strain for the conventional grey and Scott industrial foam, and re-entrant Scott foam. Both conventional foams have similar behaviours, in which the Poisson's ratios are near + 0.32 for small strain and approach + 0.5 in tension and 0 in compression. The Poisson's ratios greater than 0.5 do not violate any physical law since at large strains the cell ribs became aligned, inducing anisotropy. The re-entrant Scott foam exhibits a relative minimum in Poisson's ratio at small strain. It was very difficult to obtain the same volumetric compression ratio in both re-entrant foams because of the recovery after processing; thus, each result will be

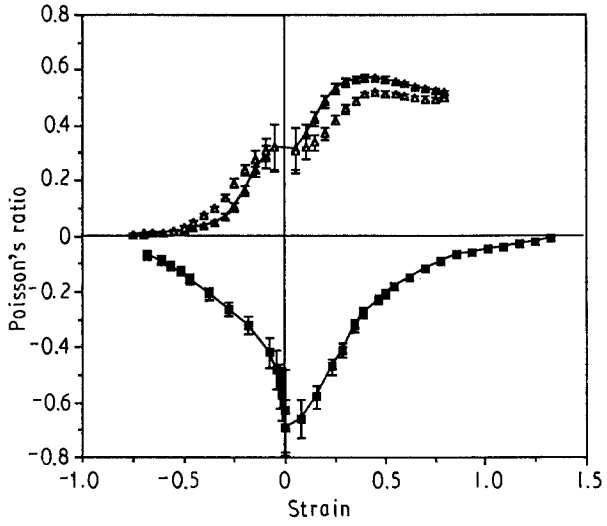

Figure 3 Poisson's ratio versus longitudinal engineering strain: (▲) conventional Scott foam, (△) conventional grey foam, (■) re-entrant Scott foam with permanent volumetric compression ratio of 3.2.

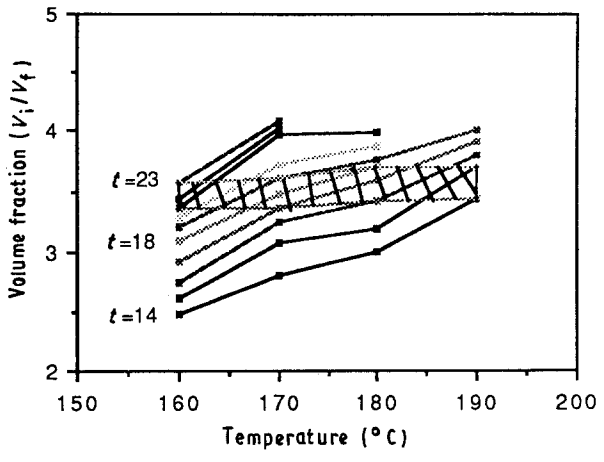

Figure 2 A plot of volumetric compression ratio versus processing temperature for several processing times t in minutes, for grey polyurethane foam (shaded region shows the best results for negative Poisson's ratio). Bottom, 14 min; top, 23 min; 1 min increments. The relative humidity in the laboratory was from 7 to 33%.

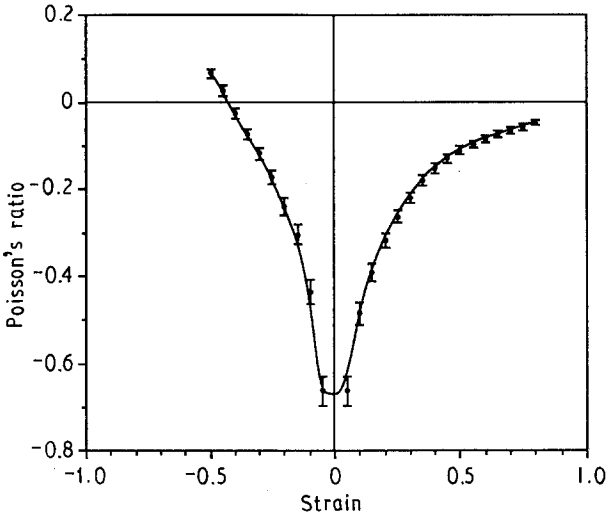

Figure 4 Poisson's ratio versus longitudinal engineering strain for grey polyurethane foam. Volumetric compression ratio of cut piece is 3.89 while that of whole block is 3.70.

described separately. Figs 4 to 6 show the curves of Poisson's ratio versus longitudinal strain for grey polyurethane foam. The points for 5% tension and 5% compression on the graph were connected via interpolation. All the graphs indicate that the Poisson's ratio is non-linearly dependent on the axial strain. This behaviour is similar to the results obtained by Evans and co-workers [6–8], even though they used a material with a very different structure. For an isotropic, non-linear elastic medium, the Poisson's function in terms of the longitudinal and lateral strains has been examined [14]. The definition of Poisson's ratio as a material constant is valid only for small strain [14] and there is a strain dependence even in materials such as rubber. So the strain dependence of Poisson's ratio in foam is not surprising. Figs 4 and 5 disclose similar negative effects for the same amounts of tension and compression. The greater asymmetry seen in Fig. 6 may be due to a variation in processing or in the material.

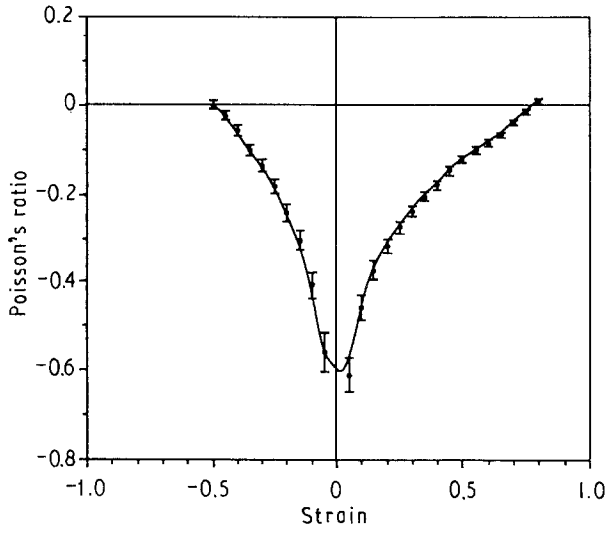

Figure 5 Poisson's ratio versus longitudinal engineering strain for grey polyurethane foam. Volumetric compression ratio of cut piece is 3.43 while that of whole block is 3.43.

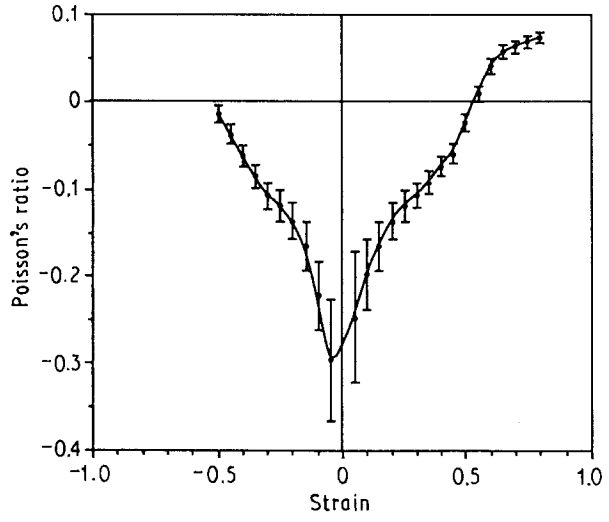

Figure 6 Poisson's ratio versus longitudinal engineering strain for grey polyurethane foam. Volumetric compression ratio of cut piece is 3.26 while that of whole block is 3.24.

The transformation was mostly concentrated on the peripheral part of the cross-section in the case of the grey foam, as seen by examining the surface of a cross-section near the central part. In the Scott industrial foam, the transformation was evenly distributed over the cross-section. A possible cause for the difference is a difference in the chemical structure of the polyurethanes. The foams also differ in that there are some closed cells in the grey foam.

The Poisson's ratio versus strain for Scott industrial foams with different volumetric compression ratios is shown in Fig. 7. These curves are similar to those for the grey polyurethane foam in that they display a minimum in Poisson's ratio at zero strain. Material prepared with a permanent volumetric compression ratio of 3.2 (also shown in Fig. 2) exhibits the best negative effect throughout the whole range of strain. Table I shows a comparison between the Poisson's ratios at small strains in tension and compression for both the Scott and the grey foams. At high volumetric compression ratios the Poisson's ratios are about the same, but at a volumetric compression ratio below 3.0, the Scott foam gives a better negative effect in Poisson's ratio.

Fig. 8 shows curves of engineering stress versus strain of conventional and re-entrant Scott industrial foams. The graphical end-points on the tensile side represent fracture of the foam at the glue joint. The end-point in compression has no significant meaning since the tests were terminated at some stage of densification. The principal difference between the conventional and re-entrant foams as obtained from the stress–strain curves in that the latter has a smaller Young's modulus (for permanent volumetric compressions less than about 3.7) and a greater resilience in the sense of a wider linear range in the stress–strain behaviour.

The results for engineering stress and strain were transformed into those of the true stress and strain using the relations $\underline{\sigma} = \sigma/(1 - \nu\varepsilon)^2$ and $\underline{\varepsilon} = \ln(1 + \varepsilon)$,

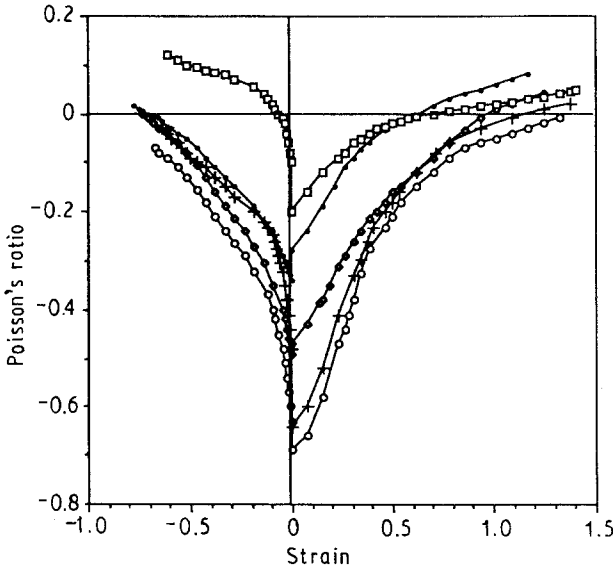

Figure 7 Poisson's ratio versus strain for Scott industrial foams having different volumetric compression ratios: (●) 2.0, (◇) 2.6, (○) 3.2, (+) 3.7, (□) 4.2.

TABLE I Poisson's ratio at each volumetric compression ratio for Scott industrial foam at a strain of 2% and grey polyurethane foam at a strain of 5%. Resilience is given in the sense of a strain range for linear behaviour, within 25% deviation from a tangent line through the origin

Volumetric compression ratio	Poisson's ratio		Strain range for linearity	
	Tension	Compression	Tension	Compression
Scott foam				
1.0	0.32	0.31	0.15	0.05
2.0	− 0.28	− 0.34	0.3	0.3
2.7	− 0.47	− 0.49	0.3	0.3
3.2	− 0.69	− 0.63	0.4	0.1
3.7	− 0.64	− 0.48	0.3	0.05
4.2	− 0.2	− 0.1	0.3	0.05
Grey foam				
1.0	0.31	0.31		
3.24	− 0.3	− 0.25		
3.44	− 0.61	− 0.56		
3.7	− 0.66	− 0.66		

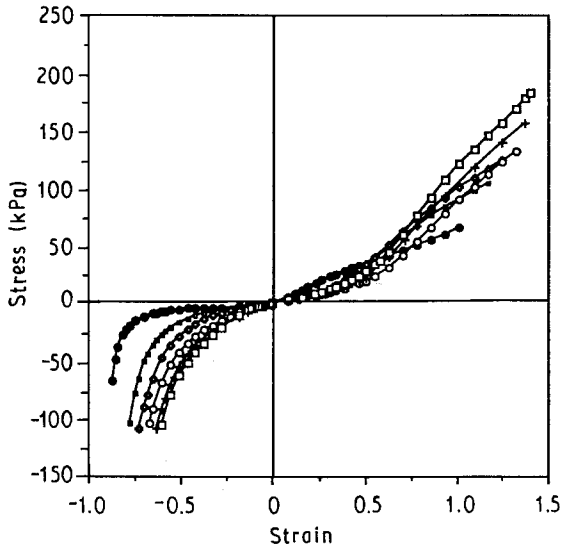

Figure 8 Engineering stress versus strain for various volumetric compression ratios of Scott industrial foam: (●) 1.0, (□) 2.0, (◇) 2.6, (○) 3.2, (+) 3.7, (□) 4.2.

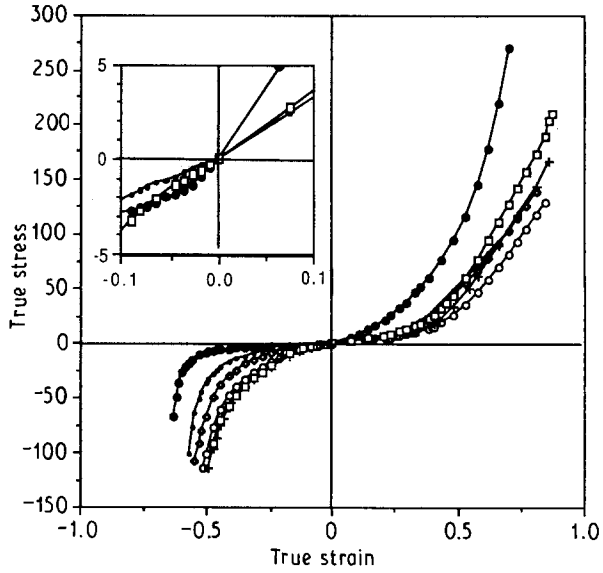

Figure 9 True stress versus true strain for various volumetric compression ratios of Scott industrial foam: (●) 1.0, (●) 2.0, (△) 2.6, (○) 3.2, (+) 3.7, (□) 4.2. Inset graph for small strain discloses the compressive non-linearity of the conventional foam.

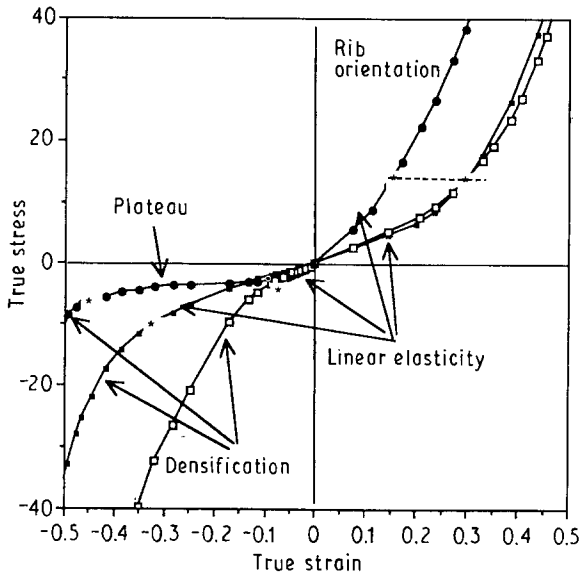

Figure 10 Deformation mechanism map with stress–strain curves for Scott industrial foam. Regions of linear elasticity, plateau and densification are demarcated by star symbols (*). Volumetric compression ratios: (●) 1.0, (□) 2.0, (□) 4.2.

in which $\underline{\sigma}$ is true stress, $\underline{\varepsilon}$ true strain, σ engineering stress, ε engineering longitudinal strain and ν Poisson's ratio. In the case of ordinary material with a positive Poisson's ratio, the true stress becomes larger than the engineering stress in tension and lower in compression; this situation is reversed for materials with negative Poisson's ratios. Fig. 9 shows the curves of true stress versus true strain. The insert graph at the upper left discloses the compressive non-linearity of the conventional foam at small strain; by contrast the re-entrant foams are linear in this strain range.

Selected stress–strain results of Fig. 9 are replotted in Fig. 10 on an expanded scale, with regions associated with the physical mechanisms for deformation identified. This is a deformation mechanism map [1]. In the region of linear elasticity, stress and strain are proportional; this arises from the bending of the cell ribs. In the plateau region, the foam collapses in compression with little or no increase in stress; the cause is elastic buckling of the ribs in elastomeric foams such as those considered here. In the region of densification, the compressive stress–strain curves increase in slope as a result of contact between cell ribs. A similar increase in slope occurs in tension, as the cell ribs become aligned and begin to stretch, which requires more force than bending. The re-entrant foams do not exhibit any plateau region since the ribs are already convoluted and continue to bend rather than buckle; instead, they exhibit an extended region of linear elasticity, or resilience. This form of resilience is maximum for a volumetric compression ratio of 2 as shown in Table I; for higher values densification begins to occur sooner, since the relative density starts at a higher value. As for the deformation mechanism responsible for the negative Poisson's ratio, the cells in

the foam were observed to unfold during deformation as presented previously [5].

An important application of foam is in packaging and cushioning. Relevant foam characteristics in this context are the Young's modulus and the total energy absorption during deformation. Energy absorption capacities of the foam materials studied here were determined from the areas under the stress-strain curves and are shown in Figs 11 and 12 in compression and tension, respectively. From such energy-absorption diagrams [15] for any given allowable applied stress, one can determine the maximum energy per unit volume which can be absorbed without exceeding a selected stress. The re-entrant foams differ from the conventional ones in that for re-entrant foam the initial stiffness (Young's modulus) is lower, but the energy density is higher at large deformation, as a result of the non-linear behaviour. Energy absorption can also be increased by using conventional foam of higher density, but the stiffness will also be higher and that is not always desirable.

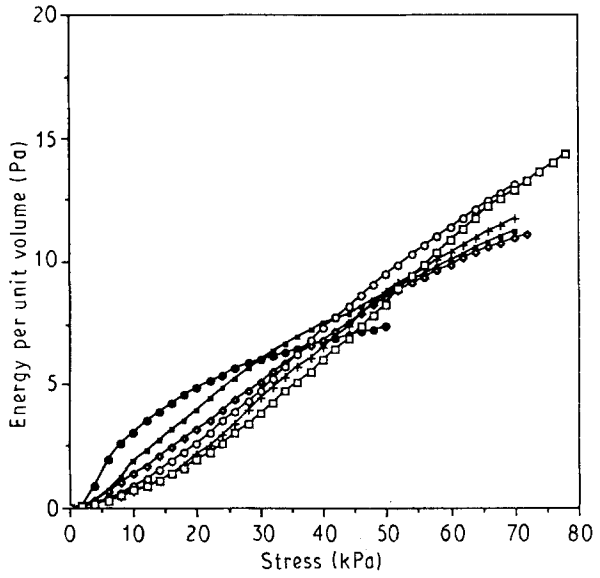

Figure 11 Energy absorbed per unit volume versus compressive stress for various volumetric compression ratios of Scott industrial foam: (●) 1.0, (□) 2.0, (◇) 2.6 (○) 3.2, (+) 3.7, (□) 4.2.

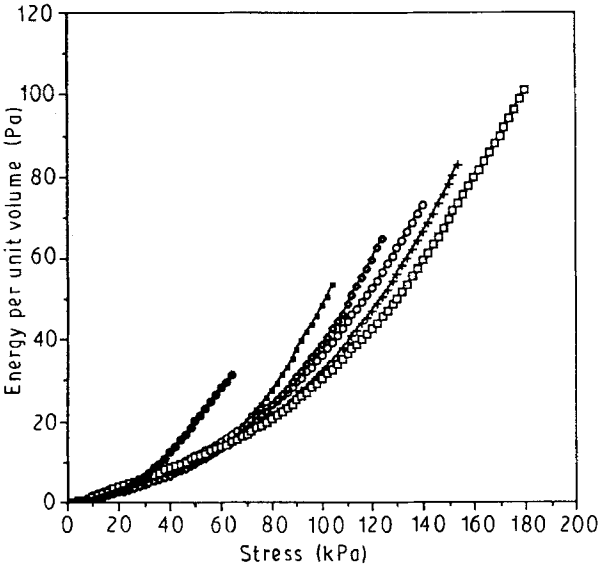

Figure 12 Energy absorbed per unit volume versus tensile stress for various volumetric compression ratios of Scott industrial foam: (●) 1.0, (□) 2.0, (◇) 2.6, (○) 3.2, (+) 3.7, (□) 4.2.

The behaviour of cellular solids is determined by relative density, physical properties of matrix polymer, cell shape and cell size. In the present experiments both cell shape and density were changed by the transformation process; the cell size was reduced slightly. The effect of relative density dramatically affects stiffness and strength and has been thoroughly documented [1]. Conventional foam of higher density and identical composition was not available for comparison in this study. The effect of cell size is still not fully understood. The effect of cell size was claimed theoretically and demonstrated experimentally to be negligible by some authors [15–17], whereas others [18, 19] consider that there is an effect of cell size on the strength as well as the thermal properties. However, studies of conventional foam in which relative density was the only variable [1] disclose a Poisson's ratio near + 0.3 and essentially independent of density, and for open-cell foam, a Young's modulus proportional to the square of the density. Such behaviour differs substantially from that of the re-entrant foam.

As for toughness, defined as the energy per unit volume to fracture, the toughness of the re-entrant foam as shown in Fig. 12 increased with volumetric compression ratio by a factor of 1.7, 2.1, 2.3, 2.6 and 3.2, compared to that of the conventional foam, at volumetric compression ratios of 2.0, 2.6, 3.2, 3.7 and 4.2, respectively.

The shear modulus was calculated using the relation $G = E/2(1 + \nu)$ assuming the foam material to be isotropic. Fig. 13 shows the variation of normalized Young's modulus, normalized shear modulus and Poisson's ratio versus volumetric compression ratio in tension and compression at a strain of 2%. The

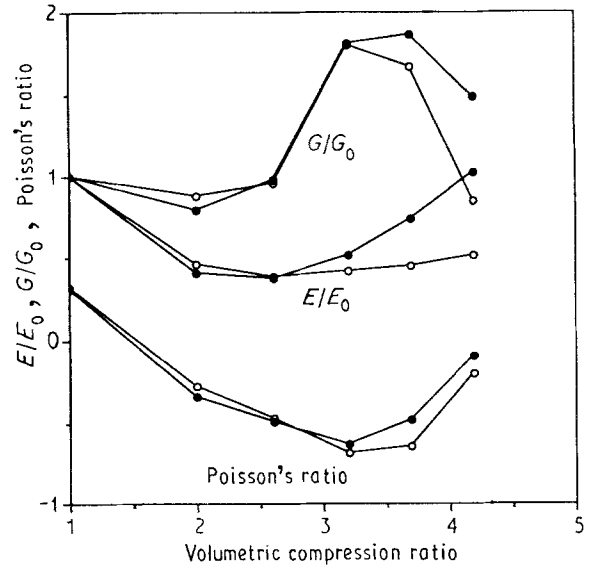

Figure 13 Measured Young's modulus and Poisson's ratio; calculated shear modulus versus volumetric compression ratio at a strain of 2% in both tension and compression for Scott industrial foam: (○) tension; (●) compression. E_0 = 68 kPa in tension, 47 kPa in compression.

moduli were normalized by dividing by the values for the conventional foam, which corresponds to a permanent volumetric compression ratio of 1. Re-entrant Scott industrial foam has a maximum shear modulus near a permanent volumetric compression ratio of 3.2 in tension and 3.7 in compression. At a ratio of 3.2, the material showed the best negative effect in Poisson's ratio; it displays a minimum Young's modulus near a permanent volumetric compression ratio of 2.6 in both tension and compression.

All the above results were for foam of the same starting density. Other starting densities may result in different behaviour.

As for possible applications, foamed polymers are used extensively for cushioning, load distribution and energy absorption. Polyurethane foam is good in such applications. The comfort of a cushion [20] has been related to the resilience in the sense of a wide range of strain over which the behaviour is linear or nearly so. Re-entrant foam would appear to be advantageous in this regard. Another possible application is a press-fit fastener. The fastener, which is made bigger than a hole by a proper amount, is pressed into the hole; the negative Poisson effect causes lateral contraction which facilitates insertion [21]. Similarly the Poisson effect resists removal of the fastener. It is also anticipated that negative Poisson's ratio materials may find uses as shock-absorbing material, sponges, sandwich-panel core and others.

4. Conclusions

1. The best negative Poisson's ratio effects were obtained for a final volumetric compression ratio of 3.3 to 3.7. Transformation at 170 °C for 17 min gave good results for both kinds of foam; other combinations also were successful.

2. Scott industrial foam was easier to convert to negative Poisson's ratio material than an alternate grey polyurethane foam.

3. Poisson's ratio depended on axial strain and reached a relative minimum at small strain. The smallest value observed was -0.7, for both kinds of foam.

4. Increasing permanent volumetric compression gave rise to a relative minimum in Poisson's ratio, a relative minimum in Young's modulus, and a relative maximum in the shear modulus.

5. The toughness of re-entrant foam in tension increased with volumetric compression ratio; it increased by a factor of 3.2 at a volumetric compression ratio of 4.2.

6. The resilience of the foam was greatest for a volumetric compression ratio of 2.0.

Acknowledgements

Support of this research by the NSF, and by a University Faculty Scholar Award to RSL, is gratefully acknowledged. The hospitality of the Department of Engineering Mechanics at the University of Wisconsin, where a portion of this work was conducted, is also acknowledged.

References

1. L. J. GIBSON and M. F. ASHBY, "Cellular Solids" (Pergamon, Oxford, 1988) pp. 120–168.
2. S. P. TIMOSHENKO, "History of Strength of Materials" (Dover, New York, 1983) pp. 216–217, 248–249.
3. A. E. H. LOVE, "A Treatise on the Mathematical Theory of Elasticity" (Dover, New York, 1944) p. 13.
4. O. G. INGLES, I. K. LEE and R. C. NEIL, *Rock Mechan.* **5** (1973) 203.
5. R. S. LAKES, *Science* **235** (1987) 1038.
6. K. E. EVANS, *J. Phys. D: Appl. Phys.* **22** (1989) 1870.
7. B. D. CADDOCK and K. E. EVANS, *ibid.* **22** (1989) 1877.
8. K. E. EVANS and B. CADDOCK, *ibid.* **22** (1989) 1883.
9. S. P. TIMOSHENKO and J. N. GOODIER, "Theory of Elasticity" (McGraw-Hill, New York, 1982) p. 398.
10. R. E. PETERSON, "Stress Concentration Factors" (Wiley, New York, 1974) p. 137.
11. E. A. FRIIS, R. S. LAKES and J. B. PARK, *J. Mater. Sci.* **23** (1988) 4406.
12. "Annual Book of ASTM Standards", E 8M-85 (1986).
13. *Idem.*, E 9-81 (1986).
14. M. F. BEATTY and D. O. STALNAKER, *J. Appl. Mech.* **53** (1986) 807.
15. S. K. MAITI, L. J. GIBSON and M. F. ASHBY, *Acta Metall.* **32** (1984) 1963.
16. K. C. RUSCH, *J. Appl. Polym. Sci.* **13** (1969) 2297.
17. E. Q. CLUTTON and G. N. RICE, in Proceedings of 20th International Conference on Cell. Polym., London, 20–22 March 1991 (Rubra Technology).
18. F. A. SHUTOV, *Adv. Polym. Sci.* **51** (1983) 155.
19. E. A. BLAIR, "Resinography of Cellular Plastics", ASTM Special Publication No. 414 (1967) p. 84.
20. J. W. HARTINGS and J. H. HAGAN, *J. Cell. Plast.* **14** (1978) 81.
21. J. B. CHOI and R. S. LAKES, *J. Cell. Polym.* in press.

Received 29 April
and accepted 13 May 1991